

Available online at www.sciencedirect.com

ScienceDirect

journal homepage: www.elsevier.com/locate/radcr

Case Report

Malignant gastrointestinal neuroectodermal tumor of the ileum: A case report and review of imaging characteristics ☆

Tatsuki Miwa, MD^{a,*}, Bunta Tokuda, MD^b, Osamu Sato, MD, PhD^a, Mizuki Honda, MD^c, Tetsuya Imura, MD, PhD^c, Kazuhiro Katada, MD, PhD^d, Toshiya Ochiai, MD, PhD^e, Kei Yamada, MD, PhD^b

^a Department of Radiology, North Medical Center of Kyoto Prefectural University of Medicine, 481 Otokoyama, Yosanocho, Yosagun, Kyoto 629-2261, Japan

^b Department of Radiology, Kyoto Prefectural University of Medicine, 465 Kajii-cho, Kamigyo-ku, Kyoto 602-8566, Japan

^c Department of Pathology, North Medical Center of Kyoto Prefectural University of Medicine, 481 Otokoyama, Yosanocho, Yosagun, Kyoto 629-2261, Japan

^d Department of Gastroenterology, North Medical Center of Kyoto Prefectural University of Medicine, 481 Otokoyama, Yosanocho, Yosagun, Kyoto 629-2261, Japan

^e Department of Surgery, North Medical Center of Kyoto Prefectural University of Medicine, 481 Otokoyama, Yosanocho, Yosagun, Kyoto 629-2261, Japan

ARTICLE INFO

Article history:

Received 29 January 2025

Accepted 7 February 2025

Keywords:

Malignant gastrointestinal
neuroectodermal tumor (MGNET)
Ileum
Gastrointestinal mesenchymal
tumor
CT
MRI

ABSTRACT

Malignant gastrointestinal neuroectodermal tumors (MGNETs) are extremely rare malignant mesenchymal tumors derived from ectodermal neural cells of the gastrointestinal tract that most commonly arise in the small intestine. Preoperative diagnosis is challenging owing to the lack of well-established imaging characteristics. Here, we report the case of a 50-year-old female patient with MGNET of the ileum. Computed tomography revealed a highly lobulated hypervascular mass and circumferential wall thickening in the distal ileum, whereas magnetic resonance imaging revealed marked diffusion restriction. A laparoscopic ileal resection was performed. The patient remained recurrence-free for 1 year without additional treatment. Specific imaging characteristics observed in our case, including the combined pattern of wall thickening and submucosal mass formation, marked diffusion restriction, and highly lobulated appearance, may aid in differentiating MGNET from other tumors.

© 2025 The Authors. Published by Elsevier Inc. on behalf of University of Washington.

This is an open access article under the CC BY-NC-ND license

(<http://creativecommons.org/licenses/by-nc-nd/4.0/>)

☆ Competing Interests: The authors declare that they have no known competing financial interests or personal relationships that could have appeared to influence the work reported in this paper.

* Corresponding author.

E-mail address: sanlunshu31@gmail.com (T. Miwa).

<https://doi.org/10.1016/j.radcr.2025.02.029>

1930-0433/© 2025 The Authors. Published by Elsevier Inc. on behalf of University of Washington. This is an open access article under the CC BY-NC-ND license (<http://creativecommons.org/licenses/by-nc-nd/4.0/>)

Introduction

Malignant gastrointestinal neuroectodermal tumors (MGNETs) are extremely rare malignant mesenchymal tumors derived from ectodermal neural cells of the gastrointestinal tract. MGNET most commonly arises in the small intestine, and approximately 110 cases have been reported to date. Comprehensive imaging studies are limited, and differentiating MGNET from other small intestinal tumors using imaging studies is challenging. In this report, we present a case of MGNET of the ileum that was difficult to diagnose preoperatively and discuss the imaging features of MGNET based on this case and previously published literature.

Case description

A 50-year-old woman with a 2-month history of fatigue visited a local hospital. Clinical examination suggested an abdominal mass on palpation, and the patient was referred to our hospital for further examination. Blood test results revealed anemia with a hemoglobin level of 6.8 mg/dL, an elevated inflammatory response (white blood cell count of $8.9 \times 10^3/\mu\text{L}$ and C-reactive protein of 6.0 mg/dL), and hypoalbuminemia with an albumin level of 2.7 g/dL. Tumor markers, including CEA, CA19-9, and sIL-2R, were negative.

Computed tomography revealed a highly lobulated submucosal mass, approximately 5 cm in diameter, with circumferential wall thickening in the distal ileum, contiguous with the ileal lumen, and exhibiting ulceration (Fig. 1). The tumor was hypervascular, with blood supplied from the branches of the ileal and omental arteries, and early venous return to the mesenteric vein was observed. Magnetic reso-

nance imaging showed nonspecific intermediate signal intensity on T1-weighted imaging and moderate hypointensity on T2-weighted imaging, along with marked diffusion restriction on diffusion-weighted imaging, with an apparent diffusion coefficient (ADC) value averaging $0.8 \times 10^{-3} \text{ mm}^2/\text{s}$ (Fig. 2). Hyperintense areas on T2-weighted imaging were observed within the tumor, suggesting cystic degeneration. Although the highly lobulated nature of the tumor and its marked diffusion restriction were atypical, a gastrointestinal stromal tumor (GIST) was considered the most likely diagnosis. No lymph node or distant metastases were observed.

A laparoscopic ileal resection was performed. Intraoperatively, a distorted mass was detected, approximately 10 cm from the distal end of the ileum. No disseminated lesions were observed. The gross appearance showed a white tumor, $62 \times 42 \text{ mm}$ in size, partially surrounding the small intestinal wall. Histologically, dense proliferation of round-shaped to spindle-shaped tumor cells with a nested pattern was observed, extending from the lamina propria to subserosa, with partial protrusion into the mucosal surface and circumferential distribution within the muscularis propria along the short axis of the intestine. Cystic degeneration was also observed in the tumor. Capillary-rich stroma was also observed. Immunohistochemically, the tumor was positive for SOX10, S100, and CD56, with very focal positivity for synaptophysin. In contrast, markers characteristic of GIST, such as CD117, CD34, and DOG-1, were negative. Additionally, cytokeratin, which is positive in epithelial tumors, and desmin, which is positive in smooth muscle tumors, were negative. Melanocyte markers, such as HMB-45 and Melan-A, were also negative. Subsequently, split fluorescence in situ hybridization revealed translocation of the EWSR1 gene (22q12), confirming the diagnosis of MGNET (Fig. 3). All resection margins were negative, and no lymph node metastases were observed. The patient remained recurrence-free for 1 year without additional treatment.



Fig. 1 – Axial (A) and coronal (B) contrast-enhanced computed tomography images of the pelvis show a highly lobulated, hypervascular tumor located in the terminal ileum, which measures approximately 5 cm in diameter (arrows). The tumor exhibits circumferential wall thickening and forms a mass that protrudes outward.

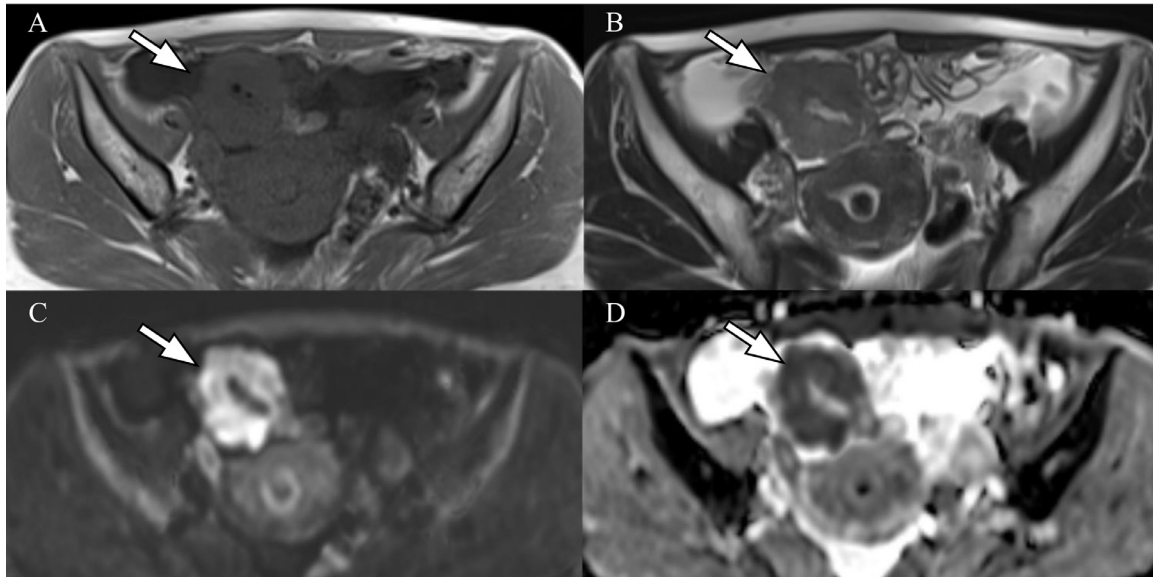


Fig. 2 – Magnetic resonance imaging of the pelvis shows that the tumor exhibits intermediate signal intensity on T1-weighted imaging (A), moderate hypointensity on T2-weighted imaging (B), marked diffusion restriction with hyperintensity on diffusion-weighted imaging (C), and diffusion restriction on the apparent diffusion coefficient (ADC) map (D) (arrows). The average ADC value is $0.8 \times 10^{-3} \text{ mm}^2/\text{s}$.

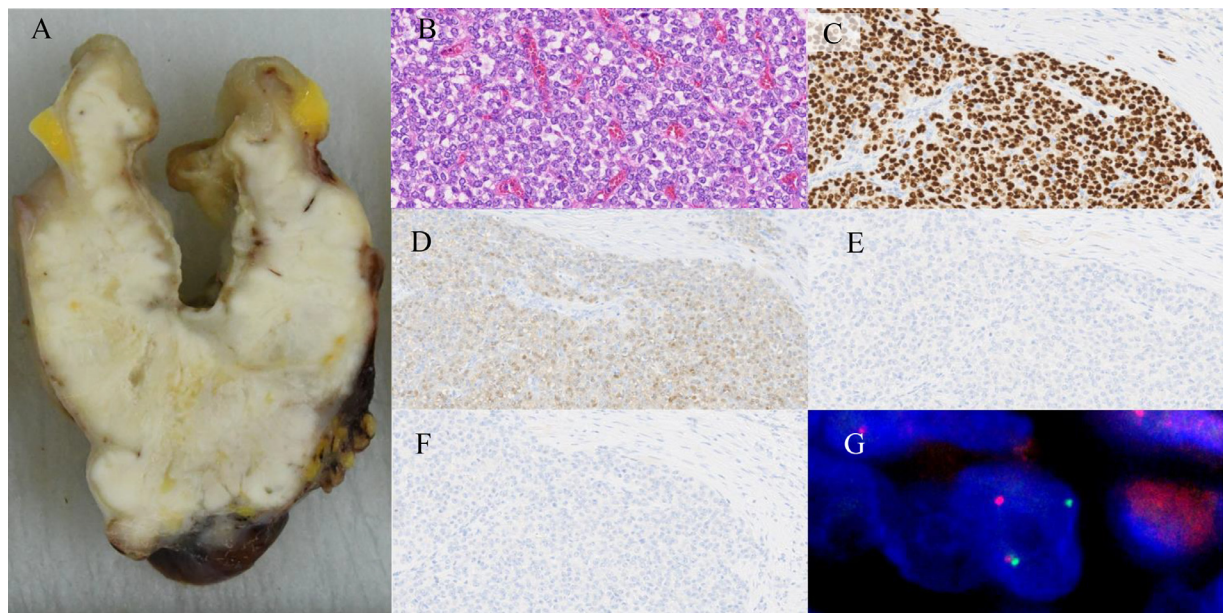


Fig. 3 – Gross appearance of the resected mass (A) shows a white tumor $62 \times 42 \text{ mm}$ in size, partially surrounding the intestinal wall. Histologically, dense proliferation of round-shaped to spindle-shaped tumor cells with capillary-rich stroma is observed (Hematoxylin and eosin, $\times 200$) (B). Immunohistochemical staining shows strong positivity for SOX10 (C) and S100 (D), whereas melanocyte markers such as HMB-45 (E) and Melan-A (F) are negative. Fluorescence in situ hybridization (G) demonstrates the translocation of the EWSR1 gene (22q12).

Discussion

MGNET was first reported by Zambrano in 2003 as “clear cell sarcoma of the gastrointestinal tract” and was reclassified as “MGNET” by Stockman in 2012 owing to immunohisto-

logical differences, such as lack of any specific markers of melanocytic differentiation [1]. Stockman hypothesized that MGNET is derived from autonomic nervous system-related primitive cells of the neural crest that show a neural line of differentiation, with a complete absence of melanocytic features [1].

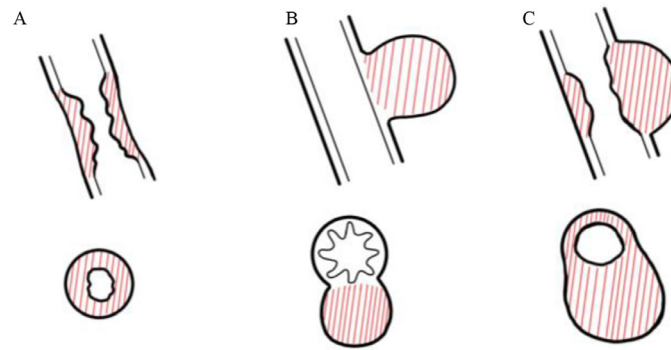


Fig. 4 – Schema illustrating the 3 imaging patterns of malignant gastrointestinal neuroectodermal tumor. (A) Wall thickening pattern, (B) mass formation pattern, and (C) combined pattern of wall thickening and mass formation.

The age of onset ranges from 5 to 82 years, with a tendency to affect relatively young to middle-aged adults with an average age of 36 years [2]. Most reports suggest no sex differences; however, some reports indicate a slight female predilection with a 1:1.5 ratio [1,2]. Approximately 90% of tumors arise in the gastrointestinal tract, most frequently in the small intestine (62.5%), followed by the stomach (25%) and colon (12.5%), with a particular predilection for the ileum within the small intestine [1,2]. In addition to the gastrointestinal tract, tumors have been reported in the bronchi, head and neck, and heart [3–5].

Common clinical manifestations include abdominal pain, intestinal obstruction, anorexia, hemorrhage, and weight loss. This tumor is an aggressive malignancy with rapid progression; 43%–55% of patients present with metastatic disease in the liver or lymph nodes at diagnosis, and the median overall survival has been reported to be 10 months [2]. Surgery is the treatment of choice for localized disease, whereas chemotherapy is considered when surgery is not feasible or distant metastasis occurs; however, standard treatment protocols have not been established.

MGNET typically presents as a lobulated mass located in the gastrointestinal wall, with an average tumor size of approximately 4.5 cm [2]. The tumor is centered within the muscularis propria, often extending into the submucosa and subserosa; in some cases, it protrudes into the lumen or invades extragastrointestinal tissues, such as the omentum and mesentery [6]. Tumors are often associated with necrosis, hemorrhage, cystic degeneration, and mucosal surface ulceration. Histological examination reveals pseudoepithelial, oval, and spindle-shaped tumor cells that proliferate in various patterns, including pseudoalveolar, pseudopapillary, microcystic, schema-like, bundled, and rosette-like patterns. Immunohistochemically, the tumor is characterized by positivity for S100 and SOX10, while melanocyte markers such as HMB-45 and Melan-A are negative. Molecularly, MGNET is characterized by chimeric fusion proteins, such as EWSR1-ATF1 and EWSR1-CREB1, resulting from chromosomal rearrangements of t(12;22)(q13;q12) and t(2;22)(q33;q12), which can be diagnosed using split fluorescence in situ hybridization [1,2]. Peripheral primitive neuroectodermal tumors, another type of tumor of peripheral neuroectodermal origin and a member

of the Ewing family of tumors, are characterized by fusion genes such as *EWSR-FLI1* and *EWSR-ERG*. Insabato et al. [7] suggested that MGNET and peripheral primitive neuroectodermal tumors share biological properties and may partially have the same histogenesis, based on their experience with MGNET in a patient with a prior history of Ewing sarcoma. However, further studies are required to determine whether they belong to the same tumor spectrum or represent distinct entities.

Imaging findings for MGNET have not been well established. In our case, the tumor exhibited a combination of mass lesions, gastrointestinal wall thickening, marked diffusion restriction, and a highly lobulated appearance. A review of 21 cases of MGNETs in the gastrointestinal tract, including 20 cases from the literature and our case, revealed 3 major distinct patterns: wall thickening, mass formation, and a combination of wall thickening and mass formation (Fig. 4, Table 1) [2,8–22]. The wall-thickening type (6/21, 29%) can be complicated by intestinal obstruction due to contractile changes when the lesion is circumferential (3/6, 50%). The mass-formation type (10/21, 48%) arises submucosally and grows exophytically, often with internal necrosis. The combined pattern of wall thickening and mass lesions (5/21, 24%), as in our case, tends to result in a larger tumor size than the other patterns. This combined pattern might represent an advanced stage of the tumor, possibly developing from the mass-formation or wall-thickening patterns as the tumor progresses.

Lesions in the small intestine did not show any differences in the frequencies of the aforementioned patterns. In contrast, lesions in the esophagus, stomach, and duodenum were of the mass-formation type. There was no correlation between the imaging patterns and local invasion or metastasis at the time of diagnosis or prognosis. Among the 20 cases from the literature, 11 cases included descriptions of contrast-enhanced computed tomography findings [2,11,17–22]. Of these, 10 demonstrated heterogeneous contrast enhancement, whereas one showed homogeneous contrast enhancement. Two of the 11 cases exhibited hypervascular features, similar to our case [19,21]. In our case, capillary-rich stroma was confirmed histologically, which appeared to correspond to the hypervascular features observed on contrast-enhanced computed tomography. Although this hypervascu-

Table 1 – Summary of clinical and imaging findings in 21 reported cases of malignant gastrointestinal.

| Authors | Age (y) | Sex | Location | Imaging pattern | Tumor size (cm) | Local invasion | Metastasis at diagnosis | Clinical outcome |
|-----------------------------|---------|-----|------------------|------------------------------------|-----------------|----------------|-------------------------|--|
| Njima et al. [8] | 20 | F | Small intestine | Wall thickening | 3.0 × 2.5 | No | No | Lymph node metastasis at 11 mo |
| Saeed et al. [9] | 45 | M | Jejunum | Wall thickening | N/A | No | No | Reccurence at 12 mo |
| Jia et al. [10] | 49 | M | Distal ileum | Wall thickening | 3.5 | No | Lymph nodes | Liver and right femur metastasis at 6 mo, thoracic vertebrae metastasis at 12 mo, death at 15 mo |
| Morani et al. [11] (Case 1) | 56 | F | Jejunum | Wall thickening (with obstruction) | N/A | No | N/A | N/A |
| Sasaki et al. [12] | 69 | M | Jejunum | Wall thickening (with obstruction) | 10 (diameter) | No | Lymph nodes | N/A |
| Huang et al. [13] | 30 | F | Distal ileum | Wall thickening (with obstruction) | 3.5 × 2.0 × 1.8 | Omentum | No | No reccurence at 6 mo |
| Morani et al. [11] (Case 4) | 42 | F | Small intestine | Mass | N/A | No | Liver, Lymph nodes | N/A |
| Baccaro et al. [14] | 79 | F | Ileum | Mass | 3 | No | No | No reccurence at 6 mo |
| Li et al. [2] (Case 2) | 62 | F | Ileocecal | Mass | 4 | No | Liver | Alive at 6 mo |
| Morani et al. [11] (Case 2) | 26 | F | Bowel | Mass | N/A | Uterus | N/A | N/A |
| Kim et al. [15] | 21 | M | Distal esophagus | Mass | 3.5 × 3.5 | No | No | No reccurence at 5 mo |
| Song et al. [16] | 23 | M | Distal esophagus | Mass | 2.5 × 4.5 | No | No | No reccurence at 2 y |
| Morani et al. [11] (Case 3) | 46 | F | Stomach | Mass | N/A | No | Liver | Death at 1 y |
| Sivasubramaniam et al. [17] | 46 | F | Stomach | Mass | 2.4 × 3.0 | No | No | Lymph node metastasis at 17 mo |
| Li et al. [2] (Case 1) | 17 | M | Stomach | Mass | 6.0 × 5.0 × 5.0 | No | No | No reccurence at 10 mo |
| Founier et al. [18] | 73 | F | Duodenum | Mass | 4.5 × 3.5 × 3.5 | No | No | No reccurence at 6 mo |
| Wang et al. [19] | 30 | F | Jejunum | Wall thickening+ Mass | N/A | No | Liver | Alive at 1 y |
| Bosoteanu et al. [20] | 67 | M | Jejunum | Wall thickening+ Mass | 12 × 8.5 × 14.5 | Sigmoid colon | Liver, Lymph nodes | Death at 6 wk |
| Mishra et al. [21] | 32 | M | Proximal ileum | Wall thickening+ Mass | 6.0 × 3.5 × 1.0 | No | No | No reccurence at 20 mo |
| Zhao et al. [22] | 33 | F | Ileum | Wall thickening+ Mass | 6.1 × 4.0 | Omentum | No | N/A |
| Our case | 50 | F | Ileum | Wall thickening+ Mass | 6.2 × 4.2 | No | No | No reccurence at 1 y |

N/A, not available.

larity might represent a characteristic radiological and pathological feature of MGNET, the limited number of reported cases and the lack of studies on this aspect make it difficult to draw conclusions. Further studies are required to determine whether hypervascularity is a consistent feature of MGNET.

Differential diagnoses for MGNET include GISTs, neuroendocrine tumor (NETs), malignant lymphomas, and adenocarcinomas. Among the 3 imaging patterns of MGNET, the wall-thickening type may be difficult to distinguish from malignant lymphomas or adenocarcinomas, whereas the mass-formation type may be particularly challenging to differentiate from GISTs. However, the combined pattern of wall thickening and mass formation is uncommon in other diseases and may be a characteristic of MGNET.

Detailed reports on magnetic resonance imaging findings of MGNETs are scarce. In our case, the ADC value was

$0.8 \times 10^{-3} \text{ mm}^2/\text{s}$, which may reflect dense tumor cell proliferation. Previous studies have reported ADC values to be $0.9\text{--}1.3 \times 10^{-3} \text{ mm}^2/\text{s}$ for GISTs [23,24] and $0.96\text{--}1.24 \times 10^{-3} \text{ mm}^2/\text{s}$ for NETs [25], suggesting that MGNETs may have a relatively lower ADC value than both GISTs and NETs. In contrast, small intestinal malignant lymphomas have been reported to have ADC value of $0.6\text{--}0.7 \times 10^{-3} \text{ mm}^2/\text{s}$, which appears to be lower than that of MGNETs [26]. The ADC value for adenocarcinomas has been reported to be approximately $0.83 \times 10^{-3} \text{ mm}^2/\text{s}$, showing little difference from our case [26].

Although several reports have noted that MGNETs exhibit a lobular morphology, detailed descriptions of this feature are lacking [1]. In our case, the tumor exhibited a highly lobulated morphology, with small nodules protruding from its surface. This feature is uncommon in other tumors and may be useful for differentiating MGNET.

Conclusion

MGNET is an extremely rare and aggressive submucosal tumor of the gastrointestinal tract, most commonly arising in the small intestine, with a tendency to affect relatively young adults and is associated with a poor prognosis. Diagnosing MGNET can be challenging because its imaging features overlap with those of other gastrointestinal tumors. However, the specific imaging characteristics observed in our case, including the combined pattern of submucosal mass formation and wall thickening, marked diffusion restriction, and highly lobulated appearance, may aid in differentiating MGNET from other tumors.

Patient consent

Written informed consent was obtained from the patient for publication of this case report and accompanying images.

REFERENCES

- Stockman DL, Miettinen M, Suster S, Spagnolo D, Dominguez-Malagon H, Hornick JL, et al. Malignant gastrointestinal neuroectodermal tumor: clinicopathologic, immunohistochemical, ultrastructural, and molecular analysis of 16 cases with a reappraisal of clear cell sarcoma-like tumors of the gastrointestinal tract. *Am J Surg Pathol* 2012;36(6):857–68. doi:10.1097/PAS.0b013e31824644ac.
- Li R, Cao J, Chen L, Cui F, Chen S, Feng Z, et al. Malignant gastrointestinal neuroectodermal Tumors: clinicopathological and prognostic features of 96 patients. *Onco Targets Ther* 2020;13:9731–40. doi:10.2147/OTT.S275633.
- Zheng Q, Chen H, Li Y. Primary gastrointestinal-type clear cell sarcoma-like tumor of the bronchus: a hitherto unreported bronchial tumor. *J Thorac Oncol* 2019;14(9):e202–5. doi:10.1016/j.jtho.2019.04.030.
- Kuo CT, Kao YC, Huang HY, Hsiao CH, Lee JC. Malignant gastrointestinal neuroectodermal tumor in head and neck: two challenging cases with diverse morphology and different considerations for differential diagnosis. *Virchows Arch* 2022;481(1):131–6. doi:10.1007/s00428-022-03274-y.
- Li Z, Pu X, He L, Fu Y, Li L, Xu Y, et al. Malignant gastrointestinal neuroectodermal tumor in the right heart: a report of an extremely rare case presenting with a cardiac mass. *Front Cardiovasc Med* 2021;1(8):702215. doi:10.3389/fcvm.2021.702215.
- Chang B, Yu L, Guo WW, Sheng WQ, Wang L, Lao I, et al. Malignant gastrointestinal neuroectodermal tumor clinicopathologic, immunohistochemical, and molecular analysis of 19 cases. *Am J Surg Pathol* 2020;44(4):456–66. doi:10.1097/PAS.0000000000001396.
- Insabato L, Guadagno E, Natella V, Somma A, Bihl M, Pizzolorusso A, et al. An unusual association of malignant gastrointestinal neuroectodermal tumor (clear cell sarcoma-like) and Ewing sarcoma. *Pathol Res Pract* 2015;211(9):688–92. doi:10.1016/j.prp.2015.06.001.
- Njima M, Lahbacha B, Jabra SB, Moussa A, Bellalah A, Abdeljelil NB, et al. Small intestine gastrointestinal clear cell sarcoma: a case report and review of the literature. *J Investig Med High Impact Case Rep* 2024;12:23247096231225869. doi:10.1177/23247096231225869.
- Saeed S, Grezenko H, Nisar L, Rehman A, Riyaz A, Cook DE, et al. A rare but aggressive malignancy: a case report of a gastrointestinal neuroectodermal tumor (GNET). *Cureus* 2023;15(7):e41509. doi:10.7759/cureus.41509.
- Jia Y, Yan Y, Hebbard P, Garvin G, Lu MV. Malignant gastrointestinal neuroectodermal tumor (GNET) mimicking small bowel lymphoma: a case report. *Cureus* 2024;16(4):e59105. doi:10.7759/cureus.59105.
- Morani AC, Ramani NS, Yedururi S, Prasad SR. Malignant gastrointestinal neuroectodermal tumor: a new kid on the block? *J Compt Assist Tomogr* 2022;46(5):676–81. doi:10.1097/RCT.0000000000001350.
- Sasaki M, Tanaka M, Asukai K, Koguchi H, Inoue Y, Moriyama M, et al. Malignant gastrointestinal neuroectodermal tumor presenting with small intestinal obstruction: a case report. *DEN Open* 2022;2(1):e119. doi:10.1002/deo2.119.
- Huang GX, Chen QY, Zhong LL, Chen H, Zhang HP, Liu XF, et al. Primary malignant gastrointestinal neuroectodermal tumor occurring in the ileum with intra-abdominal granulomatous nodules: a case report and review of the literature. *Oncol Lett* 2019;17(4):3899–909. doi:10.3892/ol.2019.10060.
- Baccaro C, Zorzetti N, Cuoghi M, Fornelli A, Franceschini T, Coluccelli S, et al. Malignant Gastrointestinal Neuroectodermal Tumor: A Case Report and Literary Review for a Rare Differential Diagnosis. *Surgeries* 2023;4(2):235–45. doi:10.3390/surgeries4020024.
- Kim SB, Lee SH, Gu MJ. Esophageal subepithelial lesion diagnosed as malignant gastrointestinal neuroectodermal tumor. *World J Gastroenterol* 2015;21(18):5739–43. doi:10.3748/wjg.v21.i18.5739.
- Song SH, Shin JH, Ryu HJ, Kim DJ, Park SY. Successful surgical treatment of a recurrent esophageal malignant gastrointestinal neuroectodermal tumor. *Korean J Thorac Cardiovasc Surg* 2018;51(2):142–5. doi:10.5090/kjtcs.2018.51.2.142.
- Sivasubramaniam P, Tiegs-heiden CA, Sturgis CD, Hagen CE, Hartley CP, Thangiah JJ. Malignant gastrointestinal neuroectodermal tumor: cytologic, histologic, immunohistochemical, and molecular pitfalls. *Ann Diagn Pathol* 2021;55:151813. doi:10.1016/j.anndiagpath.2021.151813.
- Fournier A, Deslauriers V, Giguere CC, Borduas M, Collin Y. Malignant duodenal gastrointestinal neuroectodermal tumor (GNET): case report and review of the literature. *Int J Surg Case, Rep* 2024;123:110195. doi:10.1016/j.ijscr.2024.110195.
- Wang Y, Chen T, Lu X, Zhang B. Malignant gastrointestinal neuroectodermal tumor in the small intestine with liver metastasis: first case report worldwide. *Asian J Surg* 2020;43(7):769–72. doi:10.1016/j.asjsur.2020.02.006.
- Boşoteanu M, Cristian M, Aşchie M, Baz RA, Zielonka AM, Cozaru GC, et al. The malignant gastrointestinal neuroectodermal tumor (GNET): a distinct entity and the challenging differential diagnosis with mesenchymal, lymphoid, and melanin tumors: a case report and brief review of the literature. *Diagnostic (Basel)* 2023;16(6):1131. doi:10.3390/diagnostics13061131.
- Mishra P, Biswas D, Pattnaik SA, Patra S, Muduly DK, Balasubramanian V, et al. Malignant gastrointestinal neuroectodermal tumor: a case-based review of literature. *J Cancer Res Ther* 2022;18(4):885–97. doi:10.4103/jcrt.JCRT_829_19.
- Zhao Z, Zhang D, Li W, Zhang L, Li Z, Zhou J. Primary malignant neuroectodermal tumor of the ileum with

- predominantly uncommon pseudopapillary architecture. *Int J Clin Exp Pathol* 2014;7(12):8967–71.
- [23] Yu MH, Lee JM, Baek JH, Han JK, Choi BI. MRI features of gastrointestinal stromal tumors. *AJR Am J Roentgenol* 2014;203(5):980–91. doi:[10.2214/ajr.13.11667](https://doi.org/10.2214/ajr.13.11667).
- [24] Yoo J, Kim SH, Han JK. Multiparametric MRI and 18F-FDG PET features for differentiating gastrointestinal stromal tumors from benign gastric subepithelial lesions. *Eur Radiol* 2020;30(3):1634–43. doi:[10.1007/s00330-019-06534-9](https://doi.org/10.1007/s00330-019-06534-9).
- [25] Adams LC, Bressemer KK, Brangsch J, Reimann C, Nowak K, Brenner W, et al. Quantitative 3D assessment of 68Ga-DOTATOC PET/MRI with diffusion-weighted imaging to assess imaging markers for gastroenteropancreatic neuroendocrine tumors: preliminary results. *J Nucl Med* 2020;61(7):1021–7. doi:[10.2967/jnumed.119.234062](https://doi.org/10.2967/jnumed.119.234062).
- [26] Afifi AH, Ela AMA, Alanna A. Feasibility of diffusion weighted magnetic resonance imaging in evaluation of different small bowel pathology. *Egypt J Radiol Nucl Med* 2015;46:859–69. doi:[10.1016/j.ejrm.2015.08.017](https://doi.org/10.1016/j.ejrm.2015.08.017).